

# Poly [2-(cinnamoyloxy)ethyl methacrylate-co-octamethacryl-POSS] nanocomposites: Synthesis and properties



A.B.V. Kiran Kumar<sup>a,b</sup>, T. Daniel Thangadurai<sup>a,c</sup>, Yong-Ill Lee<sup>a,\*</sup>

<sup>a</sup> *Anastro Laboratory, Department of Chemistry, Changwon National University, Changwon 641-773, Republic of Korea*

<sup>b</sup> *Department of Chemistry, Kongju National University, Kongju 314-701, Republic of Korea*

<sup>c</sup> *Department of Nanotechnology, College of Engineering, Sri Ramakrishna Institutions, N.G.G.O. Colony (post), Vattamalaipalayam, Coimbatore, Tamilnadu, 136 702, India*

## ARTICLE INFO

### Article history:

Received 28 November 2012

Received in revised form 6 May 2013

Accepted 15 May 2013

Available online 5 June 2013

### Keywords:

Nanocomposites

POSS

Copolymerization

Optical properties

Thermal properties

## ABSTRACT

Poly [2-(cinnamoyloxy)ethyl methacrylate-co-octamethacryl-POSS] nanocomposites were synthesized from octamethacryl-POSS and 2-(cinnamoyloxy)ethyl methacrylate (CEM) by free radical polymerization. The chemical structures and morphologies of these nanocomposites were determined by FTIR, <sup>29</sup>Si NMR, energy-dispersive spectroscopy (EDS), X-ray powder diffraction (XRD), and scanning electron microscopy (SEM) techniques. The XRD data showed that the materials were amorphous in nature, indicating that POSS formed an aggregate instead of a crystalline form in the polymer matrix. The POSS-CEM nanocomposites exhibited high thermal stability. Excitation and emission of the CEM-incorporated POSS nanocomposites, studied in the solid state, exhibited blue emission with CIE (x, 0.178; y, 0.137) coordinates, in addition to an emission intensity that increased with increasing CEM (monomer) concentration.

© 2013 Elsevier Ltd. All rights reserved.

## 1. Introduction

Incorporating inorganic blocks into organic polymers has attracted great interest as a method of introducing desirable properties into materials [1–6]. From the resulting synergy of specific organic and inorganic components, nanocomposites may exhibit unusual combinations of properties. Polyhedral oligomeric silsesquioxane (POSS) reagents are emerging as new chemical feed stocks for the preparation of organic–inorganic nanocomposites [7,8]. The inorganic POSS class of compounds has a well-defined structure with a silica-like core (Si<sub>8</sub>O<sub>12</sub>) surrounded by eight organic corner groups (functional or inert) [9] that may include amines, norbornenes, acrylates, styrenes, epoxides, siloxanes, and urethanes [9–14]. Incorporation of nanosized POSS cores into a polymer matrix can result in significant improvements in a variety of physical and mechanical properties [7,15].

Polymethacrylates have a total of four flexible bonds per monomer unit, while polyacrylates have three flexible bonds, and polystyrene has only two such bonds, since rotation of the benzene ring about the bond connecting it to the polymer backbone does not give a configurationally distinguishable orientation [16]. Cross linkers based on methacryl groups lead to more flexible networks than those based on acrylate. Recently, cinnamoyloxyethyl methacrylate

(CEM), a hydrophobic monomer, has been used to manufacture new oil-absorptive polymers via different types of chemical crosslinkers and irradiation techniques [17]. Radical polymerization is a frequently employed method for the preparation of copolymers, and knowledge of the reactivity ratios of monomers is key to predicting the composition and structure of the resultant copolymer.

POSS units have recently attracted considerable interest due to improvements they offer in quantum efficiency and the suppression of aggregation in photoluminescence (PL) and electroluminescence (EL) studies of conjugated polymers such as polyfluorenes and poly(*p*-phenylenevinylene)s [18–20]. The use of POSS units for nanocomposites or nanoparticles in EL devices has been explored [21–23]. The synthesis of highly efficient luminescent polyaromatic octasilsesquioxanes and the optical properties of polyaromatic octasilsesquioxanes containing tetraphenyl chromophores have also been reported [22,24]. Kawakami and Imae reported a fully carbazole-substituted POSS and the enhancement of its PL properties over those of poly(9-vinylcarbazole) [25]. Various applications of nanocomposites or nanoparticles with POSS units for EL devices have been reported by various research groups [21–25]. Cinnamic acid and its derivatives are considered suitable compounds for photo-induced chemical reactions due to their intramolecular charge transfer (ICT) behavior upon excitation [26].

In the present paper, we report the facile synthesis and characterization of octamethacryl-POSS- and cinnamoyl acrylate-based nanocomposites. Furthermore, we introduce a rationale for

\* Corresponding author. Tel.: +82 55 213 3436; fax: +82 55 213 3439.

E-mail address: [yilee@changwon.ac.kr](mailto:yilee@changwon.ac.kr) (Y.-I. Lee).

enhanced thermal stability and emission intensity from the insertion of an organic moiety into POSS polymers.

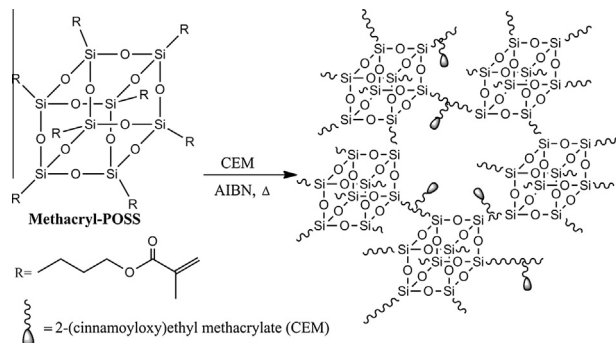
## 2. Results and discussion

Nanocomposites of POSS-CEM were synthesized using radical co-polymerization techniques. The desired POSS-CEM co-polymers were synthesized using a different CEM wt% with respect to POSS as shown in Scheme 2 (experimental details may be found in Section 3). Earlier reports revealed that POSS cages could be incorporated into polymers using either single or multiple polymerizable functional groups. POSS cages with a single polymerizable group (pendent or end) on a linear polymer backbone led to composites and multifunctional groups on polymer chains with star-like 3D structures, which exhibited improved thermal and mechanical properties [27]. In the present investigation, an organic moiety was inserted as a co-monomer into POSS polymers to study changes in the properties of the copolymer products.

Structures of the resulting POSS-CEM nanocomposites were characterized using FTIR spectroscopy. FTIR spectra showed a strong, symmetric Si–O–Si stretching absorption band at  $1128\text{ cm}^{-1}$ , which is the characteristic absorption peak of silsesquioxane cages (Fig. 1). The existence of this Si–O–Si stretching band confirmed that the POSS cage was incorporated into the nanocomposites. Moreover, an absorption band at  $1500\text{ cm}^{-1}$  originated from the skeletal vibration of aromatic rings, and stretching absorption bands of methylene groups were observed at  $2940\text{ cm}^{-1}$  [28]. The characteristic absorption peak at  $1731\text{ cm}^{-1}$  was assigned to a carbonyl stretching vibration. Furthermore, the presence of a  $\nu_{\text{O-H}}$  vibration peak at  $3440\text{ cm}^{-1}$ , which is not observed in pure CEM, indicated the existence of residual silanol groups and confirmed the presence of POSS groups in the POSS-CEM nanocomposites. In addition, characteristic bands for methyl and methylene groups were observed at  $\sim 3000\text{ cm}^{-1}$ .

Structural confirmation of the newly synthesized POSS-CEM nanocomposites was determined by  $^{29}\text{Si}$  NMR spectroscopy (Fig. 2). The chemical shift values around  $-69.47\text{ ppm}$  (for 10 and 20 wt% CEM-POSS nanocomposites; see Fig. 2a and b) and  $-69.62\text{ ppm}$  (for 30 and 50 wt% CEM-POSS nanocomposites; see Fig. 2c and d) clearly confirmed the presence of silicon atoms in a different chemical environment compared with pure POSS ( $-67.8\text{ ppm}$ ) [29]. This down-field chemical shift value indicates not only an interaction between POSS and CEM, but also that the product has a uniform structure with high purity. Moreover, the chemical shift is close to that of silicon atoms in the cage structure of  $(\text{RSiO}_{1.5})_8$  [30]. This result revealed that the synthetic compound, methacryl-POSS, has a cage structure, and its structural formula should be  $(\text{C}_7\text{H}_{11}\text{O}_2)_8\text{Si}_8\text{O}_{12}$ .

TA analysis was carried out for the 20% CEM POSS nanocomposite. As shown in Fig. 3, the first weight loss of 5.6% occurred at approximately  $140^\circ\text{C}$  and could be attributed to a trace amount



Scheme 2. Synthetic scheme and network structure of the copolymers.

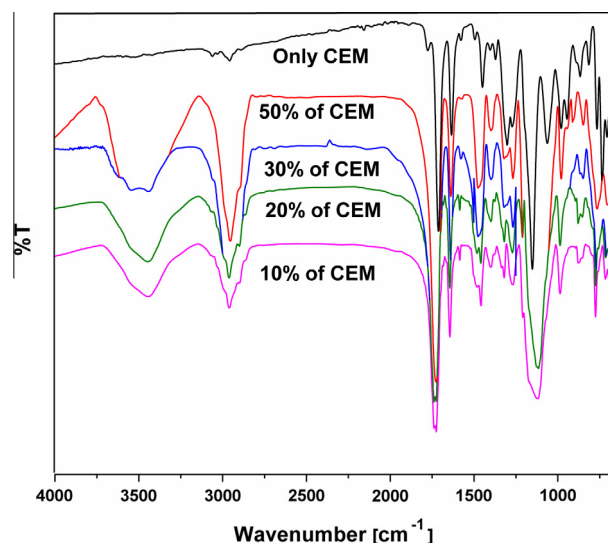


Fig. 1. FTIR spectra of pure CEM and POSS-CEM nanocomposites with 10, 20, 30, and 50 wt% CEM.

of moisture. The second weight loss of the nanocomposite occurred at approximately  $350^\circ\text{C}$  as expected, and no ceramic yield was obtained. The thermal stability of the nanocomposites was significantly enhanced with the inclusion of the inorganic component in agreement with reports from Chi et al. [31,32]. It has been proposed that the tethered structure is crucial to the improvement of the thermal stability of POSS-CEM nanocomposites [33,34]. In the current framework, POSS cages participated in the formation of a cross-linked network; i.e. the POSS cages were tethered to the polymer matrix. In addition, the nanoscale dispersion of POSS cages in the nanocomposites was also an important factor that contributed to the enhanced thermal stability. It is plausible that the mass loss from segmental decomposition via gaseous fragments could be suppressed by well-dispersed POSS cubes at the molecular level. Similar results have been found for fully exfoliated polymer-clay nanocomposites [35,36]. Therefore, POSS incorporation led to improved thermal stability of the nanocomposites.

The amorphous nature of the nanocomposites was confirmed by XRD measurements. Among the synthesized nanocomposites, the product with the least amount of CEM was in the gel state, and the remaining products were solids. The existence of solids is due to increased cross links between CEM and POSS cages. The diffraction patterns were featureless, showing only broad amorphous halos at  $2\theta = 19.23^\circ$  with a  $d$  spacing of  $4.61\text{ \AA}$  (Fig. 4), which indicates the POSS particles were well distributed within the polymer matrix, leading to the completely amorphous structure of these materials [37].

The morphologies of the POSS-CEM nanocomposites were investigated with FESEM. Fig. 5 shows the fractured surface of a nanocomposite in which no localized domains were detected. This indicates that POSS participated in the formation of cross-linked CEM networks. The surface appears to be free of visible defects and was quite smooth. No localized areas of POSS aggregates were observed on a scale of several nanometers, which suggests that the POSS component was homogeneously dispersed in the continuous matrix. EDS measurements confirmed the presence of POSS in the nanocomposites (Fig. 5d). Copper (Cu) peaks resulting from the Cu grids used to mount the samples were also observed.

Fluorescence spectra of the nanocomposites were recorded in the solid-state. Fig. 6 shows the excitation and emission curves for these nanocomposites prepared with various percentages of CEM. The excitation spectra of nanocomposite materials exhibited

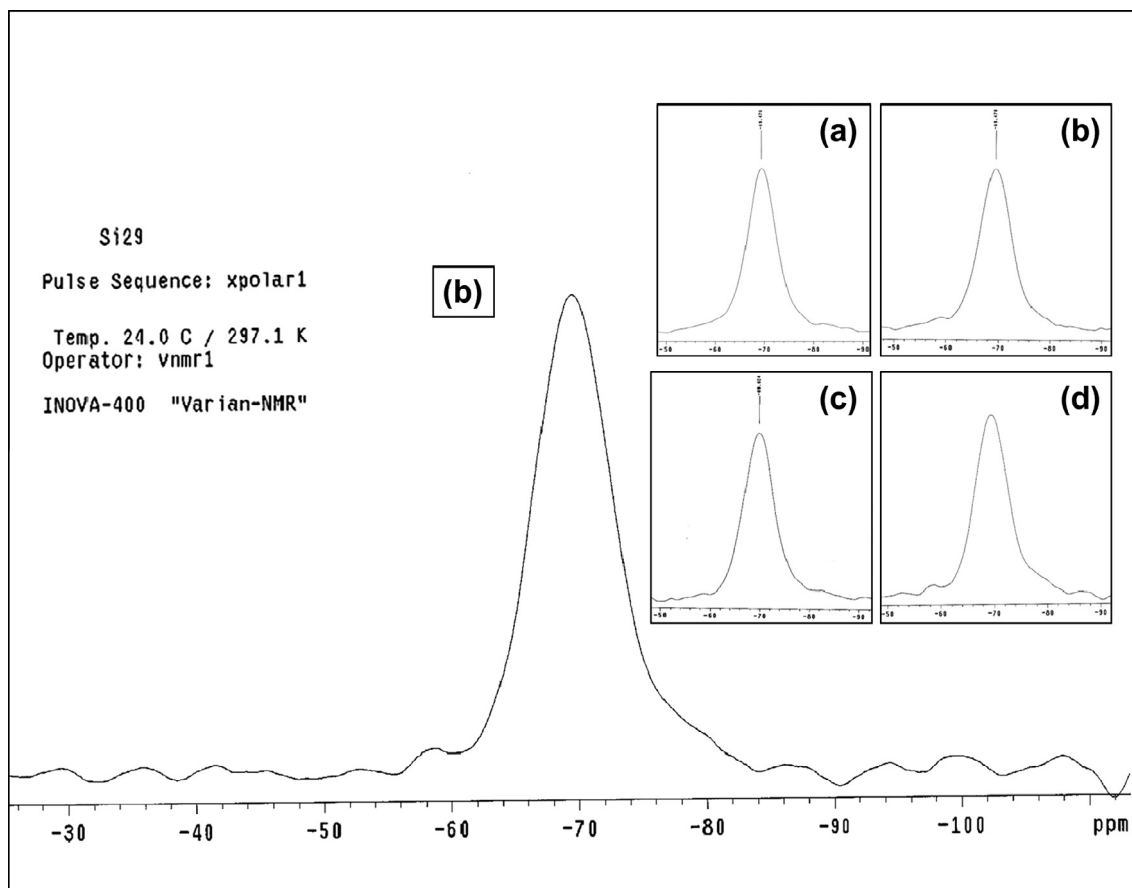


Fig. 2. Solid state  $^{29}\text{Si}$  NMR of POSS-CEM nanocomposites with (a) 10, (b) 20, (c) 30, and (d) 50 wt% CEM.

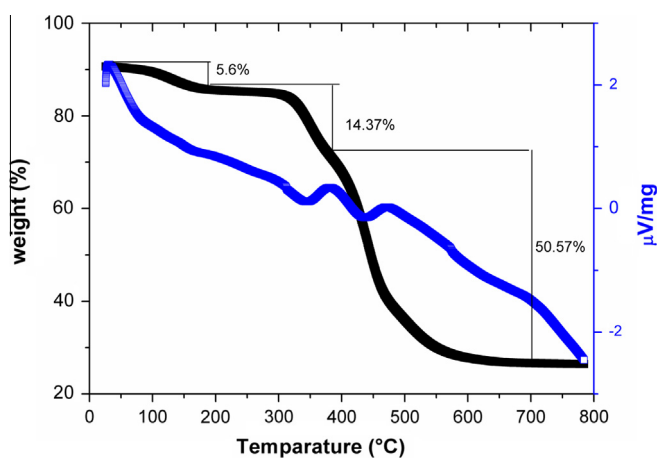


Fig. 3. TGA thermogram of the 20% CEM-POSS nanocomposite.

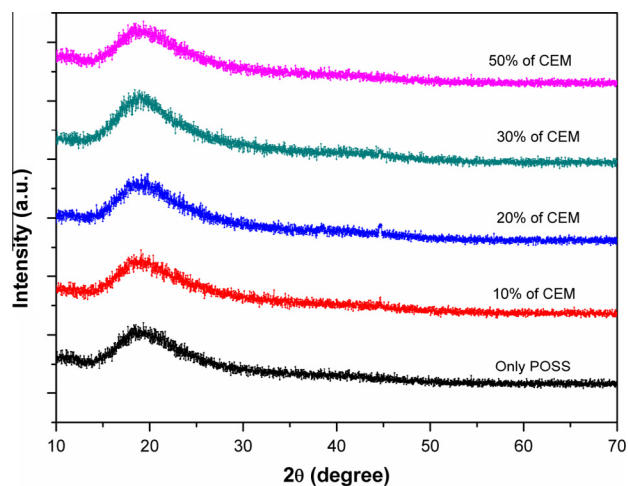


Fig. 4. XRD patterns of pure POSS and POSS-CEM nanocomposites.

a broad peak ranging from 320 to 370 nm (maximum centered at 350 nm), and emission spectra of the nanocomposites were obtained by excitation at 355 nm. The fluorescence spectra consisted of a structured band (maximum of 387 nm attributed to the chromophore) and an excimer (400–495 nm range with a maximum at 427 nm). The intensity of the excimer band increased with increasing concentrations of CEM. As expected, the appearance of a broad excimeric emission most likely resulted from an excited singlet-state fluorophore interacting with another fluorophore in the

ground state to form a fluorescent dimer or an aggregate complex. Thus, it seems reasonable to assume that formation of an intramolecular excimer occurs predominantly by a nearest-neighbor interaction, resulting in higher aggregates. Such aggregates have been observed for random graft copolymers with stilbenoid side chains on a polystyrene backbone [38]. In addition, the emission of POSS-CEM nanocomposites appeared to be blue to the naked eye as shown in the CIE ( $x$ , 0.178;  $y$ , 0.137) chromaticity diagram of Fig. 6 (inset).

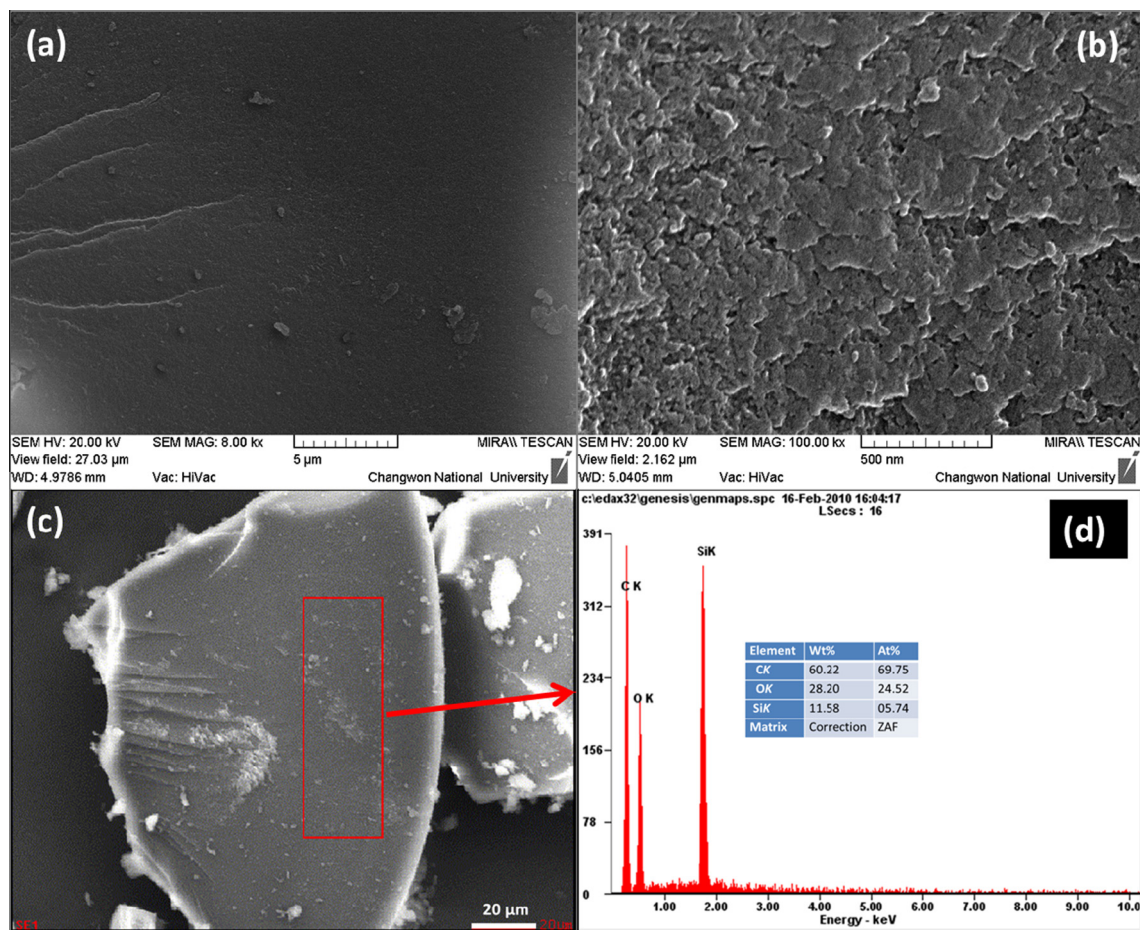


Fig. 5. Selected SEM images of nanocomposites at different magnifications (a–c) and (d) EDS spectra.

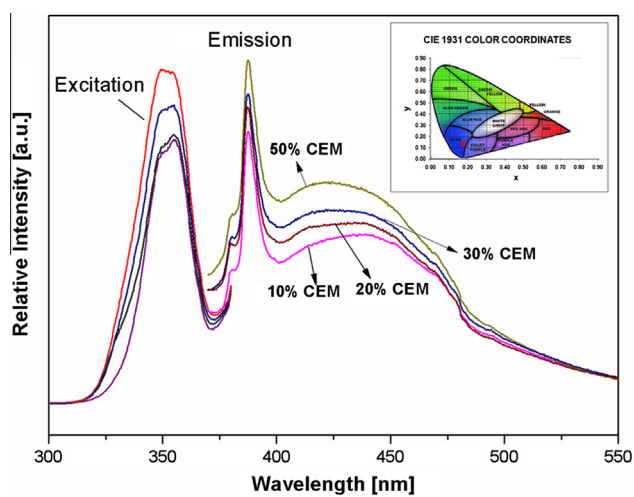
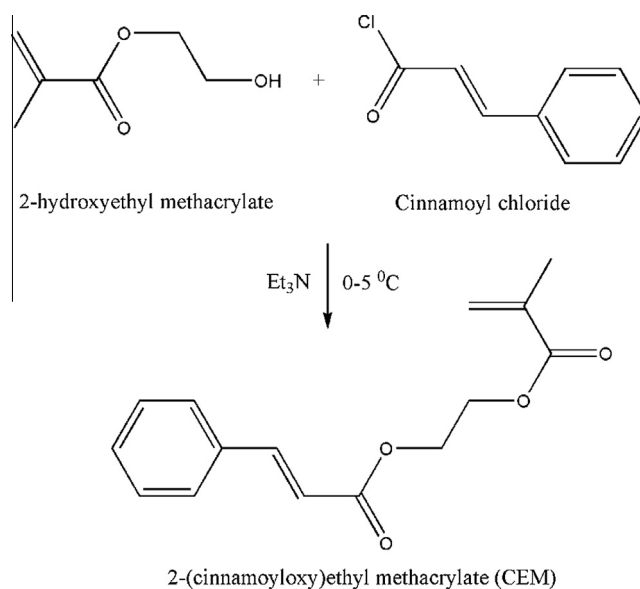


Fig. 6. Fluorescence spectra of the nanocomposites; CIE color coordinated diagram (inset).

### 3. Experimental

#### 3.1. Materials

Cinnamoyl chloride, hydroxyethyl methacrylate, azobisisobutyronitrile (AIBN) free radical initiator, 1,4-dioxane, triethylamine, and dichloromethane were purchased from Aldrich, USA. The octamethacryl-POSS was obtained from Hybrid Plastics Co., USA.



Scheme 1. Synthetic scheme for the preparation of CEM.

#### 3.2. Instrumentation and characterization

$^1\text{H}$  NMR spectra were recorded on a Bruker AVANCE-400 spectrometer with tetramethylsilane (TMS) as an internal reference.

FTIR spectra were collected on a Jasco-6300 spectrophotometer with KBr pellets. FESEM images and EDS analyses were obtained with a JSM-5610. XRD patterns were collected on an X'pert MPD-3040 diffractometer (40 mA/40 kV) using monochromated Cu K $\alpha$  radiation ( $k = 1.54 \text{ \AA}$ ) with a scanning angle range of 10–70° 2 $\theta$ . Simultaneous TGA and DTA experiments were carried out using an SDT Q600 with a heating rate of 10 K/min under a nitrogen atmosphere (flow rate: 40 ml/min). Fluorescence spectra were obtained with a Shimadzu RF-5301 PC spectrofluorophotometer.

### 3.3. Synthesis of cinnamoyloxyethyl methacrylate (CEM) (Scheme 1)

Triethylamine (23 ml, 0.22 M) was added to a 50 mL dichloromethane solution of hydroxyethyl methacrylate (26 mL, 0.2 M) under a nitrogen atmosphere in a three neck RBF fitted with a glass stirrer and was cooled in an ice bath to ~5 °C. Cinnamoyl chloride (34 g, 0.2 M) in 50 mL of dichloromethane was added dropwise via a 100 mL dropping funnel to the stirred solution over 30 min. After completion of the addition, stirring was continued for another 4 h. The accumulated triethylamine hydrochloride salt was removed by filtration, the filtrate was roto-evaporated to dryness, and the residue was purified using preparative silica gel chromatography (solvent: n-hexane: ethyl acetate; 95:5, v/v) to yield a viscous liquid.

FTIR (KBr,  $\text{cm}^{-1}$ ):  $\nu$  1713 (C=O); 1305 (CO); 3056 (Ar-H); 1633 (C=C); 2961 (CH<sub>2</sub>). <sup>1</sup>H NMR (400 MHz, CDCl<sub>3</sub>):  $\delta$  1.97 (3H, t, CH<sub>3</sub>); 4.37 (4H, m, O-CH<sub>2</sub>-); 5.57 (1H, pent =CH), 6.17 (1H, pent, =CH), 6.4 (1H, d, =CH-Ar), 7.71 (1H, d, =CH-CO-), 7.39 (5H, m, ArH); <sup>13</sup>C NMR (100 MHz, CDCl<sub>3</sub>) C<sub>15</sub>H<sub>16</sub>O<sub>4</sub>:  $\delta$  18.37 (CH<sub>3</sub>); 126.19 (=CH<sub>2</sub>); 135.94 (=C-); 166.72, 167.19 (2C=O); 62.23, 62.55 (O-CH<sub>2</sub>-); 117.5, 145.44, (HC=CH-Ar); 128.19 (2C<sub>Ar</sub>), 128.94 (2C<sub>Ar</sub>), 130.49, 134.25 (C<sub>Ar</sub>).

### 3.4. Preparation of poly [2-(cinnamoyloxy)ethyl methacrylate-co-octamethacryl-POSS]

Free radical polymerization reactions (CEM 10, 20, 30, and 50 wt% of POSS) were carried out under nitrogen protection using a vacuum-line system. Azobisisobutyronitrile (AIBN) initiator (1 wt% based on monomer) was added to a 5 mL anhydrous 1,4-dioxane solution of octamethacryl-POSS monomer (1 g) followed by 0.1 g (10% by weight of POSS) of 2-(cinnamoyloxy)ethyl methacrylate at 70 °C under a nitrogen atmosphere. The reaction was stirred for 8 h. The crude product was then poured into excess cyclohexane under vigorous agitation to dissolve unreacted monomers and to precipitate the nanocomposite. The precipitation procedure was repeated three times to attain a high yield of the product.

## 4. Conclusions

In summary, we have synthesized a novel series of CEM and methacryl POSS-CEM nanocomposites by free-radical polymerization with different CEM feed ratios. The nanocomposites were characterized by FTIR and <sup>29</sup>Si NMR. EDS spectra were used to show the presence of silicon, oxygen, and carbon in the nanocomposites. Furthermore, the incorporation of POSS greatly improved the thermal stability of the nanocomposites. In addition, the CIE coordinates ( $x$ , 0.178;  $y$ , 0.137) indicated that the nanocomposites emitted blue light over a broad region ( $\lambda_{\text{max}} = 387 \text{ nm}$ ). This study reveals a new approach to achieve novel light-emitting materials

of uniform nanoscale size with improved thermal stability, processability, absorption, and emission properties.

## Acknowledgements

This work was supported by the Basic Science Research Program (NRF 2011-0010155) and the Priority Research Centers Program (NRF 2010-0094066) through the National Research Foundation of Korea (NRF) funded by the Ministry of Education, Science and Technology.

## References

- [1] Y.-H. La, R. Sooriyakumaran, B.D. McCloskey, R.D. Allen, B.D. Freeman, R. Al-Rasheed, J. Membr. Sci. 401–402 (2012) 306–312.
- [2] D.-G. Kim, H. Kang, S. Han, J.-C. Lee, J. Mater. Chem. 22 (2012) 8654–8661.
- [3] R. Goseki, T. Hirai, Y. Ishida, M.-A. Kakimoto, T. Hayakawa, Polym. J. 44 (2012) 658–664.
- [4] Y.-L. Chu, C.-C. Cheng, Y.-P. Chen, Y.-C. Yen, F.-C. Chang, J. Mater. Chem. 22 (2012) 9285–9292.
- [5] H. Ghanbari, B.G. Cousins, A.M. Seifalian, Macromol. Rapid Commun. 32 (2011) 1032–1046.
- [6] S.S. Mahapatra, S.K. Yadav, J.W. Cho, React. Funct. Polym. 72 (2012) 227–232.
- [7] W. Zhang, A.H.E. Müller, Macromolecules 43 (2010) 3148–3152.
- [8] W. Zhang, S. Wang, J. Kong, React. Funct. Polym. 72 (2012) 580–587.
- [9] P.T. Mather, H.G. Jeon, A. Romo-Uribe, T.S. Haddad, J.D. Lichtenhan, Macromolecules 32 (1999) 1194–1203.
- [10] E. Tegou, V. Bellas, E. Gogolides, P. Argitis, Microelectron. Eng. 73–74 (2004) 238–243.
- [11] J. Wu, T.S. Haddad, P.T. Mather, Macromolecules 42 (2009) 1142–1152.
- [12] J.K. Herman Teo, K.C. Teo, B. Pan, Y. Xiao, X. Lu, Polymer 48 (2007) 5671–5680.
- [13] G. Li, L. Wang, H. Ni, C.U. Pittman, J. Inorg. Organomet. Polym. 11 (2001) 123–154.
- [14] M. Oaten, N.R. Choudhury, Macromolecules 38 (2005) 6392–6401.
- [15] D. Chen, S. Yi, P. Fang, Y. Zhong, C. Huang, X. Wu, React. Funct. Polym. 71 (2011) 502–511.
- [16] S. Rogers, L. Mandelkern, J. Phys. Chem. 61 (1957) 985–991.
- [17] A. Atta, R.M. El-Ghazawy, R. Farag, A.-A. Abdel-Azim, J. Polym. Res. 13 (2006) 257–266.
- [18] J. Lee, H.-J. Cho, N.S. Cho, D.-H. Hwang, J.-M. Kang, E. Lim, J.-I. Lee, H.-K. Shim, J. Polym. Sci. Part A: Polym. Chem. 44 (2006) 2943–2954.
- [19] C.-H. Chou, S.-L. Hsu, S.-W. Yeh, H.-S. Wang, K.-H. Wei, Macromolecules 38 (2005) 9117–9123.
- [20] S. Xiao, M. Nguyen, X. Gong, Y. Cao, H. Wu, D. Moses, A.J. Heeger, Adv. Funct. Mater. 13 (2003) 25–29.
- [21] A. Sellinger, R. Tamaki, R.M. Laine, K. Ueno, H. Tanabe, E. Williams, G.E. Jabbour, Chem. Commun. (Cambridge, UK) (2005) 3700–3702.
- [22] C.M. Brick, Y. Ouchi, Y. Chujo, R.M. Laine, Macromolecules 38 (2005) 4661–4665.
- [23] R. Tamaki, Y. Tanaka, M.Z. Asuncion, J. Choi, R.M. Laine, J. Am. Chem. Soc. 123 (2001) 12416–12417.
- [24] He, Y. Xiao, Huang, Lin, K.Y. Mya, Zhang, J. Am. Chem. Soc. 126 (2004) 7792–7793.
- [25] I. Imae, Y. Kawakami, J. Mater. Chem. 15 (2005) 4581–4583.
- [26] T.S. Singh, S. Mitra, J. Photochem. Photobiol. B 96 (2009) 193–200.
- [27] Y. Liu, K. Zeng, S. Zheng, React. Funct. Polym. 67 (2007) 627–635.
- [28] H. Xu, B. Yang, J. Wang, S. Guang, C. Li, Macromolecules 38 (2005) 10455–10460.
- [29] H. Xu, S.-W. Kuo, C.-F. Huang, F.-C. Chang, J. Appl. Polym. Sci. 91 (2004) 2208–2215.
- [30] I.E. Davidova, L.A. Gribov, I.V. Maslov, V. Dufaud, G.P. Niccolai, F. Bayard, J.M. Basset, J. Mol. Struct. 443 (1998) 89–106.
- [31] W. Zhang, X. Zhuang, X. Li, Y. Lin, J. Bai, Y. Chen, React. Funct. Polym. 69 (2009) 124–129.
- [32] H. Chi, K.Y. Mya, T. Lin, C. He, F. Wang, W.S. Chin, New J. Chem. 37 (2013) 735–742.
- [33] J. Choi, J. Harcup, A.F. Yee, Q. Zhu, R.M. Laine, J. Am. Chem. Soc. 123 (2001) 11420–11430.
- [34] J. Choi, S.G. Kim, R.M. Laine, Macromolecules 37 (2003) 99–109.
- [35] G. Lagaly, Appl. Clay Sci. 15 (1999) 1–9.
- [36] S. Sinha Ray, M. Okamoto, Prog. Polym. Sci. 28 (2003) 1539–1641.
- [37] G.S. Constable, A.J. Lesser, E.B. Coughlin, Macromolecules 37 (2004) 1276–1282.
- [38] G. Aerts, C. Wuyts, W. Dermaut, E. Goovaerts, H.J. Geise, F. Blockhuys, Macromolecules 37 (2004) 5406–5414.